Free Energy Computations on the Shift of the Special Pair Redox Potential: Mutants of the Reaction Center of *Rhodobacter sphaeroides*

J. Apostolakis,[†,§] I. Muegge,[†,||] U. Ermler,[‡] G. Fritzsch,[‡] and E. W. Knapp*[,†]

Contribution from Fachbereich Chemie, Institut Für Kristallographie, Freie Universität Berlin, Takustrasse 6, D14195 Berlin, Germany, and Max-Planck-Institut für Biophysik, Abteilung Molekulare Membranbiologie, Heinrich-Hoffmann-Strasse 7, D-60528 Frankfurt, Germany

Received October 20, 1995. Revised Manuscript Received January 16, 1996[⊗]

Abstract: Shifts of the special pair redox potential of photosynthetic reaction centers of *Rhodobacter sphaeroides* for five different mutants are considered. The shifts are calculated by the method of free energy perturbation which is based on dynamics simulation data. The influence of the orientation and the torsion potential of the acetyl group on the shift of the redox potential is investigated and compared with recent results obtained by solving Poisson's equation. In the oxidized state of the special pair the acetyl group at D_L reorients in the initial part of the dynamics simulation. As a consequence, the hydrogen bond with H(L168) breaks and the oxygen atom binds to the Mg^{2+} ion of D_M. For the mutant FY(M197) there is evidence that the acetyl oxygen atom of D_M binds to the Mg^{2+} ion of D_L instead of forming a hydrogen bond with Y(M197).

Introduction

Reaction centers (RC) catalyze the primary events of photosynthesis. Since the first three-dimensional crystal structure of RC's of the purple photosynthetic bacteria from *Rhodopseudomonas (Rps.) viridis* became available,[1,2] it was possible to understand the operation of RC's on an atomic level of description. Soon afterward the crystal structure of a second photosynthetic RC from *Rhodobacter (Rb.) sphaeroides* was determined.[3,4] Now the structure of *Rb. sphaeroides* is also available from a trigonal crystal form with a resolution of 2.65 Å.[5]

The central part of the RC of *Rb. sphaeroides* contains the following cofactors: four bacteriochlorophyll a (BChl), two of them (D_L, D_M) forming the special pair (D), two bacteriopheophytin a (BPh) (Φ_A, Φ_B), two ubiquinones UQ-10 (Q_A, Q_B), one non-heme Fe^{2+} ion, and one carotenoid. The nomenclature proposed by Hoff[6] and Deisenhofer and Michel[7] is used. The chromophores are arranged in two branches (A, B) with approximate C_2 symmetry.[2,4,8] One of the two branches (A) is active and conducts an electron from the electronically excited donor (D_L, D_M) in about 3.5 ps[9,10] to Φ_A, the pheophytin of the active branch. In another 200 ps,[11] the electron is transferred to the primary Q_A, and finally within about 100 μs, it arrives at the secondary quinone Q_B of the so-called inactive branch (B). The resulting radical pair state (D^+, Q_B^-) may recombine, but normally, it is stabilized by neutralizing the positive charge at the special pair with an electron transferred from a soluble cytochrome c_2. By blocking the electron acceptor Q_B or Q_A with a negative charge, the electron transfer back to the special pair may also occur from Q_A or Φ_A, respectively.

The electron transfer processes are driven by the difference in the redox potentials of the cofactors acting as donor and acceptor molecules. This applies also to the charge separation and charge recombination processes involving the special pair. For *Rb. sphaeroides* specific mutants have been designed which modify the special pair environment and consequently also its redox potential. Crystal structures of several mutants of *Rb. sphaeroides* are now also available.[12] They exhibit no drastic differences from the wild-type structure.

The formation of a hydrogen bond where the special pair plays the role of a hydrogen acceptor leads to an upshift of the redox potential. Correspondingly a downshift is observed if a hydrogen bond is removed. A moderate upshift of the redox potential is also observed if the protein environment at the special pair becomes less polar since it accommodates the positive charge of the oxidized special pair less efficiently.

From the electron density map of the special pair acetyl groups alone it is difficult to discriminate between the methyl group and the oxygen atom.[5] The comparison of the calculated and measured shift of the redox potentials can help to remove the uncertainty of the acetyl group orientation. By calculating the redox potentials of the special pair for different mutants one can understand better how the protein environment tunes

[†] Freie Universität.
[‡] Max-Planck-Institut für Biophysik.
[§] Biochemisches Institut, Universität Zürich, Winterthurer Strasse 190, CH-8057 Zürich, Schweiz.
[||] Department of Chemistry, University of Southern California, Los Angeles, CA, 90089-1062.
* To whom correspondence should be addressed.
[⊗] Abstract published in *Advance ACS Abstracts,* April 1, 1996.

(1) Deisenhofer, J.; Epp, O.; Miki, K.; Huber, R.; Michel, H. *J. Mol. Biol.* **1984**, *205*, 385−398.
(2) Deisenhofer, J.; Epp, O.; Miki, K.; Huber, R.; Michel, H. *Nature* **1985**, *318*, 618−624.
(3) Chang, C.-H.; Tiede, D.; Tang, J.; Smith, U.; Norris, J.; Schiffer, M. *FEBS Lett.* **1986**, *205*, 82−86.
(4) Allen, J. P.; Feher, G.; Yeates, T. O.; Komiya, H.; Rees, D. C. *Proc. Natl. Acad. Sci. U.S.A.* **1987**, *84*, 6162−6166.
(5) Ermler, U.; Fritzsch, G.; Buchanan, S. K.; Michel, H. *Structure* **1994**, *2*, 925−936.
(6) Hoff, A. J. *The Photosynthetic Bacterial Reaction Center: Structure and Dynamics*; Breton, J., Verméglio, A., Eds.; Plenum Press: New York, 1988; pp 98−99.
(7) Deisenhofer, J.; Michel, H. *Annu. Rev. Biophys. Chem.* **1991**, *20*, 247−260.
(8) Michel, H.; Epp, O.; Deisenhofer, J. *EMBO J.* **1986**, *5*, 2445−2452.
(9) Woodbury, N. W.; Becker, M.; Middendorf, D.; Parson, W. W. *Biochemistry* **1985**, *24*, 7516−7521.
(10) Breton, J.; Martin, J. L.; Fleming, G. R.; Lambry, J. C. *Biochemistry* **1988**, *27*, 8276−8284.
(11) Kirmaier, C.; Holten, D. *Photosynth. Res.* **1987**, *13*, 225−260.
(12) Chirino, A. J.; Lous, E. J.; Huber, M.; Allen, J. P.; Schenck, C. C.; Paddock, M. L.; Feher, G.; Rees, D. C. *Biochemistry* **1994**, *33*, 4584−4593.

0002-7863/96/1518-3743$12.00/0

Table 1. Shift of E_M (mV) Evaluated from Dynamics Simulation of Free Energies[a]

no.	mutants									expt	DelPhi[b]
		mutant conformation	N_w	T_w	N_w	T_w	N_s	T_s	N_s	T_s		
		wild-type conformation	N_w	N_w	T_w	T_w	N_s	N_s	T_s	T_s		
1	YF(L162)		**48**		86		−70		26		28	**−17**
2	YF(M210)		**43**		81		−49		47		30	**100**
3	FY(M197)		26[c]	**127**	64	165		−56		40	31	**96**
4	FH(M197)			**94**		132		−53		43	125	**130**
5	FH(M197) + HF(L168)			**54**		92		−98		−2	40	**34**

[a] If no value is given, the corresponding computations have not been performed. Bold numbers refer to the favorite initial orientation of the acetyl group at D_M. The different orientations are explained in the text and the table caption of Table 2. The experimental values of the shift of the redox potential have an uncertainty of ±10 mV.[21−26] [b] Shifts of E_M are calculated by solving Poisson's equation with DelPhi.[16] The wild-type conformation N_w is used throughout. With the wild-type conformation T_w the ΔE_M values are downshifted by 5 mV. The mutant conformations of the RC are N_w for the first two mutants and T_w for the last three mutants, corresponding to the results from free energy computations marked with bold type. [c] In contrast to experimental evidence[24] the hydrogen bond between the acetyl oxygen atom at D_M and the tyrosine at residue M197 is turned off by using for the mutant structure N_w. With these acetyl group conformations for the wild-type and mutant RC computations with DelPhi provide a shift of the special pair redox potential which is $\Delta E_M = 99$ mV.

the driving energy for the functionally important electron transfer processes. Furthermore, it is instructive to see whether the special pair redox potentials of mutants can be calculated solely from the knowledge of the atomic coordinates of the wild-type structure.

Recently the shift of the redox potential at the special pair has been calculated by solving Poisson's equation with DelPhi[13−15] for 11 different mutants.[16] The orientation and the torsion potential of the acetyl groups at the special pair have been varied to test its influence on the special pair redox potential. Though the agreement with the measured shifts of the special pair redox potential is quite good, a discrimination between different orientations of the acetyl group was difficult. Nevertheless there was a hint that the acetyl oxygen atom at D_M is bonded to the Mg^{2+} ion of D_L rather than pointing away as it seems in the X-ray structure of *Rb. sphaeroides*.[5] To clarify this open question, shifts of the redox potential of the special pair are calculated by free energy perturbation[17−20] (FEP). This method differs from the evaluation of electrostatic energies by solving the Poisson equation. It uses ensembles of structures obtained from computer simulation of dynamics instead of using only one structure for each mutant and its charge state.

Since the computations are expensive only the five mutants listed in Table 1 are considered. The first three of these mutants differ from the mutants which were considered recently to calculate the shifts of the redox potential by solving Poisson's equation.[16] The first two mutants YF(L162)[21] and YF(M210)[22,23] render the protein environment of the special pair more hydrophobic, but no change in the hydrogen bonding pattern is assumed. From resonance Raman spectra there is evidence that in the third mutant, FY(M197),[24] the acetyl oxygen atom at D_M forms a hydrogen bond with the hydroxyl hydrogen atom of the tyrosine. Furthermore, the single point mutation FH(M197)[25,26] and the double mutant FH(M197) + HF(L168)[25,26] are considered. In these two mutants the acetyl oxygen atom at D_M forms a hydrogen bond with H(M197). In the double mutant the hydrogen bond to residue L168 is eliminated.

The choice of these five mutants was motivated by the following rationale. All computations of the special pair redox potential are based on the wild-type atomic partial charges for the special pair. In contrast to the mutants studied recently,[16] the mutants considered for the present study have spin densities at the special pair which do not differ significantly from the wild-type spin densities.[23] Since the spin densities correlate with the atomic partial charge distribution also, the charges at the special pair do not vary much for these mutants. Hence, the values of the special pair redox potential obtained for these five mutants are more reliable than the ones obtained before.[16] Finally, for the first three mutants considered here, the shifts of the special pair redox potential calculated by solving Poisson's equation do not agree with the measured values. It is hoped that, by removing this discrepancy using the FEP[17−20] computations in the present work, there will also be a contribution to the question of the orientations of the acetyl groups at the special pair.

Methods

Use of the Dielectric Constant. The computations of free energies are performed with the program CHARMM22[28] and its corresponding force field. The atomic partial charges from CHARMM are typically used with a dielectric constant of $\epsilon = 1$.[29] Also, the water model TIP3P[30] used in the present computations was designed for a dielectric constant of unity. To account for effects of atomic polarization, these water models have a permanent dipole moment which is closer to the value in ice (2.6 D) than to the value in the gas phase (1.85 D).[31] For the TIP3P water model the permanent dipole moment is 2.35 D. In the absence of explicit solvent molecules a distance-dependent dielectric

(13) Gilson, M. K.; Rashin, A.; Fine, R.; Honig, B. *J. Mol. Biol.* **1985**, *183*, 503−516.
(14) Klapper, I.; Hagstrom, R.; Fine, R.; Sharp, K.; Honig, B. *Proteins* **1986**, *1*, 47−59.
(15) Nicholls, A.; Honig, B. *J. Comput. Chem.* **1991**, *12*, 435−445.
(16) Muegge, I.; Apostolakis, J.; Ermler, U.; Fritzsch, G.; Lubitz, W.; Knapp, E. W. *Biochemistry* **1995**, submitted.
(17) Zwanzig, R. W. *J. Chem. Phys.* **1954**, *22*, 1420−1426.
(18) Beveridge, D. L.; DiCapua, F. M. *Annu. Rev. Biophys. Chem.* **1989**, *18*, 431−492.
(19) van Gunsteren, W. F.; Weiner, P. K. *Computer Simulations of Biomolecular Systems*; Escom: Leiden, 1989.
(20) Warshel, A.; Aqvist, J. *Annu. Rev. Biophys. Biophys. Chem.* **1991**, *20*, 267−298.
(21) Wachtveitl, J.; Farchaus, J. W.; Mathis, P.; Oesterhelt, D. *Biochemistry* **1993**, *32*, 10894−10904.
(22) Gray, K. A.; Farchaus, J. W.; Wachtveitl, J.; Breton, J.; Oesterhelt, D. *EMBO J.* **1990**, *9*, 2061−2070.
(23) Nagarajan, V.; Parson, W. W.; Davis, D.; Schenck, C. C. *Biochemistry* **1993**, *32*, 12324−12336.
(24) Wachtveitl, J.; Farchaus, J. W.; Das, R.; Lutz, M.; Robert, B.; Mattioli, T. A. *Biochemistry* **1993**, *32*, 12875−12886.
(25) Lin, X.; Murchison, H. A.; Nagarijan, V.; Parson, W. W.; Allen, J. P.; Williams, J. C. *Proc. Natl. Acad. Sci. U.S.A.* **1994**, *91*, 10265−10269.
(26) Lin, X.; Williams, J. C.; Allen, J. P.; Mathis, P. *Biochemistry* **1994**, *33*, 13517−13523.
(27) Rautter, J.; Lendzian, F.; Schulz, C.; Fetsch, A.; Kuhn, M.; Lin, X.; Williams, J. C.; Allen, J. P.; Lubitz, W. *Biochemistry* **1995**, *34*, 8130−8143.
(28) Brooks, B. R.; Bruccoleri, R. E.; Olafson, B. D.; States, D. J.; Swaminathan, S.; Karplus, M. *J. Comput. Chem.* **1983**, *4*, 187−217.
(29) Elber, R.; Karplus, M. *J. Am. Chem. Soc.* **1990**, *112*, 9161−9175.
(30) Jorgensen, W. L.; Chendrasekar, J.; Madura, J. D.; Impley, R. W.; Klein, M. L. *J. Chem. Phys.* **1983**, *79*, 926−935.
(31) Coulson, C. A.; Eisenberg, D. *Proc. R. Soc. London* **1966**, *A291*, 445−451.

constant may also be used.[32] As a consequence the molecular dynamics simulations are performed with a dielectric constant of value unity.

Alternatively for the evaluation of the electrostatic energies the program DelPhi[13−15] is used, where the same atomic partial charges are employed as in molecular dynamics simulation with CHARMM. Though the structures used in the computations with DelPhi are only energy minimized and not fully relaxed as in molecular dynamics simulations, the dielectric constant is set to unity in spatial regions occupied by protein or water atoms. This convention deviates from the usual treatment with DelPhi, where the dielectric constant in the protein has a value between 2 and 4. The present treatment corresponds to the convention of atomic partial charges used in CHARMM and facilitates a direct comparison with the results from the computation of free energies.

Using DelPhi the dielectric constant is set to 80 in the solvent regime. Though the membrane is not modeled by explicit atoms, the dielectric constant in this regime is unity, since DelPhi allows only two different values of the dielectric constant. The shifts of the redox potential calculated with DelPhi are not sensitive to the exact values of the dielectric constant used for the membrane and solvent regime.[16] In the present case, the calculated shifts of the redox potential scale with the value of the dielectric constant ϵ_p used for the protein molecule as $1/\epsilon_p$ within an accuracy of 5%, i.e. all computed shifts are a factor of 2 smaller if $\epsilon_p = 2$ instead of unity.[16] More details on the computation of electrostatic energies with DelPhi are given in ref 16.

Cutoff Distance. To save CPU time the shift cutoff condition[28] with cutoff distance $R_{off} = 7.75$ Å is used throughout. This cutoff distance is often used in the CHARMM force field.[29] In contrast to the cutoff scheme "switch" which may exhibit artifacts,[33,34] due to the fast decrease of the interaction in a small distance interval, the cutoff scheme "shift" used in the present application turns off the interactions more gradually. It has recently been found that the stability of the α-helical structure of a polypeptide can depend critically on the cutoff scheme.[34] The spherical part of the RC considered in the computer simulation of dynamics is more compact than a helix and stabilized by constraints at the surface of the sphere which prevent larger conformational changes. Nevertheless this cutoff distance is quite short and may yield a dielectric screening which is too small. In the present application, the RC structures may differ considerably only in the neighborhood of the special pair where mutations are considered. Structural fluctuations at larger distances which are not properly accounted for due to the small value of the cutoff distance may approximately cancel in the computed energy differences.

Torsion Potential of the Acetyl Groups. To investigate the bonding of the acetyl oxygen atom of D_M with the Mg^{2+} ion of D_L or alternatively the hydrogen bonding with the residue M197, the initial orientation of the acetyl group at D_M is varied for the energy minimization and the subsequent dynamics simulation. The torsion potential of the acetyl groups

$$V_{torsion}(\gamma) = k(1 - \cos 2\gamma) \tag{1}$$

possesses two minima for the in-plane orientations $\gamma = 0$ and π relative to the porphyrin plane. Reorientations of the acetyl groups are facilitated by reducing the force constant of the torsion potential. Two values of the interaction parameter k are used. The original value of the force constant in CHARMM22[28] is $k_s = 2$ kcal/mol (s = strong). It allows for minor deviations from the in-plane conformation of the acetyl group only. A smaller value $k_w = 0.5$ kcal/mol (w = weak) imposes only a weak preference for the in-plane orientation. All corresponding quantities are referred to by the subscripts s and w, respectively.

Calculation of the Redox Potential. The redox potential is normally characterized by the electrochemical midpoint potential E_M, which for the special pair charge states, reduced (D^0) and oxidized (D^+), reads

$$E_M = E(D^0) - E(D^+) + \Delta E(H_{electrode}) \tag{2}$$

The E_M is measured against the standard hydrogen electrode which contributes an extra term $\Delta E(H_{electrode})$. The shift of the midpoint potential ΔE_M between a specific mutant and the wild-type RC can be evaluated from the corresponding double difference in free energy according to Nernst's equation

$$\Delta E_M = -(E_M{}^{mut} - E_M{}^{WT}) = -\frac{\Delta G^{mut} - \Delta G^{WT}}{nF} \tag{3}$$

where

$$\Delta G^{\alpha} = G^{\alpha}(0) - G^{\alpha}(+) \tag{4}$$

referring to the reduced (0) and oxidized (+) special pair state of the wild-type (α = WT) or mutant (α = mut) RC. In expression 3, $n = 1$ is the change of elementary charge of the special pair redox states and $F = 96\,485$ C/mol is Faraday's constant. The superscript mut refers to one of the mutations listed in Table 1 and the superscript WT to the wild-type RC. As long as only the electrostatic energies of the atomic partial charges are considered, quantum chemical contributions to ΔG inherent to the different special pair charge states are not accounted for. These contributions depend only weakly on the protein environment and cancel in the double difference appearing in eq 3.

Computational Procedure to Calculate the Free Energy. The difference of free energy between the special pair charge state D^0 and D^+, ΔG^{α} (eq 4), is calculated by the FEP method[17−20] for the wild-type and all mutant RC's considered. The shift of the special pair redox potential is then calculated by using the expression 3 of double differences. Several trajectories representing ensembles at intermediate charge states are generated. Thereby the Coulomb interaction terms (denoted by h) involving atoms of the special pair are evaluated for both charge states (+, 0), yielding the values for $h^{(+)}$ and $h^{(0)}$. Different ensembles of the RC are obtained with the generalized energy function

$$H(\lambda) = H_0 + \lambda h^{(+)} + (1 - \lambda)h^{(0)} \tag{5}$$

where $\lambda \in [0,1]$ denotes the intermediate charge state of the special pair. The generalized energy function (eq 5) interpolates between the oxidized ($\lambda = 1$) and the reduced ($\lambda = 0$) special pair states. All energy terms not involving atoms of the special pair are denoted by H_0. The linear scaling of the energy terms with the λ parameter (eq 5) allows use of a simplified version of FEP to evaluate free energies.[35] Within this frame additional λ ensembles can be added to the computational procedure at any time. Furthermore, it is possible to minimize the statistical error by using the double-wide sampling method[36] where the midpoints between two λ ensembles are varied.[37] Generally, ensembles for three λ values are used: $\lambda = 0.125$, 0.5, and 0.875. In some cases, additional λ ensembles at $\lambda = 0.0$, 0.025, 0.31, 0.763, and 1.0 are generated to test the dependence of the calculated free energy values on the number of λ ensembles. The maximal deviation of free energy differences obtained in these tests was 0.3 kcal/mol. The calculated statistical error was typically below 0.1 kcal/mol. The shift of the E_M upon mutation is evaluated as double difference of free energies according to the eqs 3 and 4.

Generation of the Mutant Structures. The mutant structures are derived from the wild-type crystal structure of the RC by elementary modeling techniques. For the mutants YF(L162) and YF(M210) the hydroxyl group of the tyrosine is removed. The carbon atoms of the ring are kept in position. Only their chemical character is changed. For the mutant FY(M197) the hydroxyl group is added in idealized geometry. The ring carbon atoms remain, but their chemical character changes. For the mutants FH(M197) and HF(L168) first all side-chain atoms except the carbon atoms C_β and C_γ are removed. Then the corresponding side chain ring atoms are added in idealized geometry

(32) Petrich, J. W.; Lambry, J.-C.; Kuczera, K.; Karplus, M.; Poyart, C.; Martin, J.-L. *Biochemistry* **1991**, *30*, 3975−3987.
(33) Lau, K. F.; Alper, H. E.; Thacher, T. S.; Stouch, T. R. *J. Phys. Chem.* **1994**, *98*, 8785−8792.
(34) Schreiber, H.; Steinhauser, O. *Biochemistry* **1992**, *31*, 5856−5860.
(35) Straatsma, T. P.; McCammon, J. A. *J. Chem. Phys.* **1991**, *95*, 1175−1188.
(36) Jorgensen, W. L.; Ravimohan, C. *J. Chem. Phys.* **1985**, *83*, 3050−3054.
(37) Muegge, I.; Ermler, U.; Fritzsch, G.; Knapp, E. W. *J. Phys. Chem.* **1995**, *99*, 17917−17925.

such that the orientation of the ring plane is retained. For the mutant FH(M197) the imidazole ring plane of the histidine is flipped by 180° to form an optimal hydrogen bond of the acetyl oxygen atom with the N_ϵ nitrogen atom of the imidazole ring which is involved in the bond.

Preparations for the Computer Simulation of the Dynamics. The conditions used for the computation of the shifts of the redox potential by solving Poisson's equation are described in ref 16. The following preparations are made to perform computer simulations of the dynamics of the RC: (1) The atomic partial charges of the cofactors must be provided. The cofactors BChl and BPh are modeled in an all-hydrogen atom representation. For the amino acid residues only polar hydrogen atoms are added. All other hydrogen atoms are represented by corresponding extended atom types. (2) Water molecules are added in protein cavities and constraints are set for the energy minimization which is performed for the whole RC as described in ref 16. (3) Before the dynamics simulations are performed, a reference system in the neighborhood of the special pair is defined and its structure is annealed. More details to these three points are given below.

(1) The charge distribution of the cofactors are obtained from quantum chemical computations using the convention of Mulliken[38] to assign atomic partial charges. These computations were performed for the wild-type RC only. The atomic partial charges at the two ubiquinones have been calculated with Gaussian91.[39] The charges of the BChl's, the BPh's, the carotenoid, and the detergent molecule (LDAO) are calculated with a semiempirical INDO SCF-MO method.[40,41] The charge distributions of the neutral and positively charged special pair are taken from computations[42,43] where the crystal structure of *Rb. sphaeroides*[4] has been used. For the oxidized special pair 0.28 (0.72) of the unit positive charge is localized at D_M (D_L), respectively. The atomic partial charges of the reduced (oxidized) special pair are for the three most relevant atoms: the magnesium and the oxygen and carbon atoms of the acetyl group at D_M +0.396 (+0.414), −0.350 (−0.353), +0.307 (+0.306) and at D_L +0.395 (+0.429), −0.339 (−0.325), −0.326 (−0.325). The atomic partial charges of the other cofactors, the two accessory BChl's, the BPh's, and the carotenoid are adapted from the charges of the corresponding cofactors in *Rps. viridis*.[44]

(2) A sphere of radius 18.5 Å centered at the geometrical midpoint of the residues L168 and M197 contains the relevant part of the RC. This part of the RC is visualized in Figure 1. For the initial energy minimization all atoms of residues which are completely outside of this sphere and all non-hydrogen atoms of the special pair except the atoms of the acetyl groups are spatially fixed. Protein cavities inside the sphere are filled with water molecules by using an overlay technique[45,46] where water molecules are added if the water oxygen to protein heavy atom distance is larger than 2.8 Å. According to our experience this distance criterion is not severe, allowing water molecules to be introduced only into cavities which are large enough. In this way 203 water molecules were added to the 165 water molecules already present in the crystal structure within the sphere.

(3) After energy minimization of the whole RC the residues whose atoms are all outside of the sphere are removed. To prevent water molecules from leaving the system a spherical containment potential with a radius of 18.5 Å is used. The protein atoms outside a sphere with the same center and a radius of 16.0 Å are harmonically fixed with a force constant of $k_h = 0.1$ kcal/(mol Å^2) accounting approximately for the *B* factors of the X-ray structure analysis. The atoms of the special pair are no longer constrained. The covalent bond length of hydrogen atoms is kept constant with the program SHAKE.[47] The computer simulation of dynamics at constant temperature and the heating of the system to a given temperature are performed by using stochastic boundary conditions, where all atoms outside a sphere of radius 16.5 Å are coupled to a heat bath with a friction constant of 50 ps^{-1}.[48] The spherical part of each mutated RC is first energy minimized to relax the structure. Then a simulation of dynamics is performed where the system is heated for 50 ps to 500 K and subsequently energy minimized again. The resulting coordinates are used as a starting point for product runs at 300 K. Each trajectory of a production run has a length of 150 ps. The last 100 ps of the trajectories are used for analysis. The raw data for the free energy computation, i.e. the values of the energy terms $h^{(+)}$ (t) and $h^{(0)}$ (t) from eq 5, are stored every 20 fs. The computation of the free energies with the FEP method is explained in more detail in ref 37.

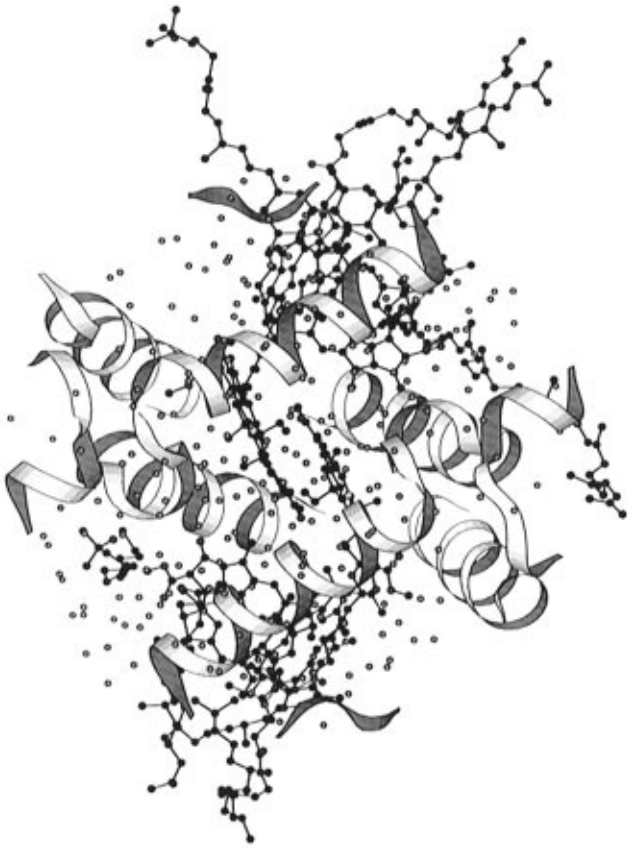

Figure 1. Relevant part of the RC of *Rb. sphaeroides*[5] for the computations of the shift of the special pair midpoint potential. The cofactors and the protein backbone atoms of all residues which have at least one heavy atom in a sphere of radius 18.5 Å centered at the geometrical midpoint of residues L168 and M197 are displayed. The lone dots represent oxygen atoms of water molecules of the crystal structure and of an overlay procedure where water molecules were added in cavities of the protein. For more details see text.

Results and Discussion

Survey of Results. Shifts of the special pair redox potential are considered for five mutants (Table 1). The positions of the mutated residues are visualized in Figure 2. It depicts the

(38) Mulliken, R. S. *J. Chem. Phys.* **1955**, *23*, 1833−1840.
(39) Frisch, M. J.; Trucks, G. W.; Head-Gordon, M.; Gill, P. M. W.; Wong, M. W.; Foresman, J. B.; Johnson, B. G.; Schlegel, H. B.; Robb, M. A.; Replogle, E. S.; Gomperts, R.; Andres, J. L.; Raghavachari, K.; Binkley, J. S.; Gonzales, C.; Martin, R. L.; Fox, D. J.; Defrees, D. J.; Baker, J.; Stewart, J. J. P.; Pole, J. A. *Gaussian 92, Revision C*; Gaussian Inc.: Pittsburgh, PA, 1992.
(40) Pople, J. A.; Beveridge, D. L. *Approximate Molecular Orbital Theory*; McGraw-Hill: New York, 1970.
(41) Dewar, M. J. S.; Hashmall, J. A.; Venier, C. G. *J. Am. Chem. Soc.* **1968**, *90*, 1953−1963.
(42) Plato, M.; Tränkle, E.; Lubitz, W.; Lendzian, F.; Möbius, K. *Chem. Phys.* **1986**, *107*, 185−196.
(43) Plato, M.; Möbius, K.; Lubitz, W. *Chlorophylls*; H. Scheer: Boca Raton, FL, 1991; pp 1015−1046.
(44) Scherer, P. O. J.; Fischer, S. F. *Chem. Phys.* **1989**, *131*, 115−127.
(45) Knapp, E. W.; Nilsson, L. *Reaction Centers of Photosynthetic Bacteria*; Michel-Beyerle, M. E., Ed.; Springer: New York, 1990; pp 437−450.
(46) Wade, R. C.; Mazor, M. H.; McCammon, J. A.; Quiocho, F. A. *Biopolymers* **1991**, *31*, 919−931.
(47) Ryckaert, J.; Ciccotti, G.; Berendsen, H. *J. Comput. Phys.* **1977**, *23*, 327−341.
(48) Brünger, A.; Brooks, C. L.; Karplus, M. *Chem. Phys. Lett.* **1984**, *105*, 495−500.

Table 2. Energy-Minimized Structures and Energetics of the Wild-Type RC for Different Orientations of the Ring I Acetyl Group at D_M

		reduced special pair		oxidized special pair	
structure[a]	remarks[a]	torsion angle[b] after energy minimization	E_{pot}[c] (kcal/mol)	torsion angle[b] after energy minimization	E_{pot}[c] (kcal/mol)
n_w	final structure	33	0.8	31	−5.03
t_w	180° rotated	−121	−6.34	−124	−14.58
N_w	earlier structure	−119	−6.43	−118	−14.65
T_w	180° rotated	41	1.05	40	−4.37
n_s	final structure	4	0.47	1	−6.04
t_s	180° rotated	−153	−4.00	−151	−11.57
N_s	earlier structure	−145	−5.12	−142	−13.22
T_s	180° rotated	11	1.05	10	−4.76

[a] n denotes the original crystal structure,[5] where the torsion angle of the ring I acetyl group at D_M is $\Phi = 7°$ before energy minimization. t denotes the crystal structure where the ring I acetyl group is rotated by 180° as compared to the structure n. As a consequence the acetyl oxygen atom points toward the Mg^{2+} ion of D_L. N denotes a preliminary crystal structure which differs from n only with respect to the acetyl group torsion angle which is $\Phi = -133°$ such that the acetyl oxygen atom points toward the Mg^{2+} ion of D_L. T denotes the crystal structure where the ring I acetyl group is rotated by 180° as compared to the structure N. The subscript w (s) refers to a weak (strong) torsion potential at the ring I acetyl groups (see eq 2). [b] After minimization of the whole system. For computational details see the text. [c] Interaction energy between the acetyl group atoms at D_M and their protein and cofactor environment.

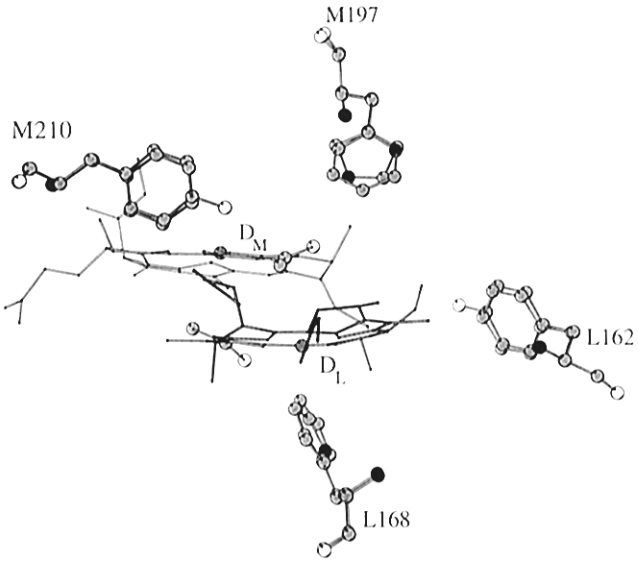

Figure 2. Special pair with four mutated residues. Energy-minimized structures from the wild-type and mutant RC of *Rb. sphaeroides*[5] are depicted. The oxygen atoms are represented by open, the nitrogen atoms by black, and the carbon atoms by gray circles. The cytochrome c_2 is located at the side of the residue L162. The active branch (A) of the RC is situated at the side of the residues M202 and M197. For the sake of clarity only the mutant FH(M197) but not the mutant FY(M197) is displayed.

energy-minimized wild-type structure of the special pair together with the mutated residues which are taken from individually minimized protein structures of the neutral RC as used for the computations with DelPhi and CHARMM. Two different methods are employed to evaluate the shifts of the special pair redox potential. In the first method the electrostatic energies of the two different special pair redox states are computed by solving Poisson's equation. The results are displayed in the last column of Table 1. In the second method the shifts of E_M are calculated by free energy differences obtained from computer simulations of the dynamics of the special pair and its protein environment of the RC using the FEP technique. Those results are also given in Table 1. Table 2 contains data on the orientation and energetics of the acetyl group at D_M after energy minimization of the wild-type RC. The structure and energetics of the acetyl groups obtained by the dynamics simulations are given in Table 3 for the wild-type RC and the mutants FH-(M197) and FY(M197). A selection of information on the orientations of both acetyl groups of the special pair is summarized in Figure 3 for the wild-type and the mutants FH-(M197) and FY(M197).

Sensitivity of the Redox Potential on the Special Pair Environment and the Hydrogen Bonding Pattern. The shift of the redox potential of the special pair senses changes in the charge distribution of the special pair environment between the wild-type and the mutant RC. The charges of the special pair interact stronger with a polar than with a nonpolar medium. Hence, $|\Delta G_{polar}| > |\Delta G_{nonpolar}|$ is valid. Since the interaction of a probe charge with a polar medium consisting of dipoles is negative on the average it follows that $\Delta G_{polar} > \Delta G_{nonpolar}$. From this inequality one can conclude that the shift of the redox potential ΔE_M should be positive, if the special pair environment is more polar for the wild-type than for the mutant RC. This is the case for the mutants YF(L162) and YF(M210) and the experimental values of the shift are positive as expected.

Larger changes of the redox potential are measured if the hydrogen bonding pattern changes between the wild-type and the mutant RC.[25−27] The negative interaction energy of an acetyl oxygen atom of the special pair involved in a hydrogen bond is not as strong for the oxidized (positive charge) as for the reduced (neutral) special pair state. Thus, the difference of free energy ΔG (eq 4) has a contribution which obeys the inequality $\Delta G_{H\text{-}bond} < 0$. This contribution is absent if the hydrogen bond is not formed. If the mutant RC has such an additional hydrogen bond compared with the wild-type RC, it follows that $\Delta G^{WT} > \Delta G^{mut}$ and the shift of the redox potential is positive. The shift is negative if the mutant RC has less hydrogen bonds than the wild-type RC. The measured values of the shift clearly demonstrate this relation.[25−27]

Hydrogen Bonding and the Orientation of the Acetyl Groups from Crystal Structure and Energy Minimization. Two keto and two acetyl oxygen atoms of the special pair BChl's can function as acceptors of hydrogen bonds. In the wild-type RC of *Rb. sphaeroides* only one hydrogen bond involving the ring I acetyl oxygen atom at D_L is present.[5] In the wild-type RC of *Rps. viridis* the special pair is involved in three hydrogen bonds. Here only the keto oxygen atom at D_M does not bind a hydrogen atom.[1,2] The number of hydrogen bonds in *Rb. sphaeroides* is varied with the last three mutants listed in Table 1. A hydrogen bond is added to the acetyl oxygen atom at D_M in the mutants where the phenylalanine at residue M197 is replaced by tyrosine or histidine. A hydrogen bond is removed from the acetyl oxygen atom at D_L in the double mutant FH(M197) + HF(168). Increasing (decreasing) the number of hydrogen bonds at the special pair leads to an upshift (downshift) of the redox potential by about 80−120 mV.

Table 3. Average Conformation and Energetics of the Acetyl Groups at the Special Pair Based on Simulations of Dynamics for Different Mutants[a]

mutant/structure/acetyl group[b]	charge[c] of special pair	torsion angle[d] (deg) mean (fluctuation)	E_{pot}[e] (kcal/mol) mean (fluctuation)	H-bond[f] (Å) mean (fluctuation)	distance to Mg^{2+} [g] (Å) mean (fluctuation)
$WT/N_w/D_L$	0.125	52° (12°)	−6.80 (1.53)	2.05 (0.13)	4.74 (0.20)
$WT/N_w/D_L$	0.875	−83° (24°)	−8.21 (1.50)	3.87 (0.66)	2.31 (0.19)
$WT/T_w/D_L$	0.125	−22° (47°)	−6.43 (1.81)	3.39 (1.08)	2.93 (0.90)
$WT/T_w/D_M$	0.125	−72° (32°)		none	2.53 (0.31)
$FH(M197)/T_w/D_L$	0.125	38° (10°)	−6.03 (1.32)	2.10 (0.20)	4.50 (0.20)
$FH(M197)/T_w/D_L$	0.875	−88° (27°)	−7.77 (2.35)	6.03 (0.60)	2.29 (0.17)
$FH(M197)/T_w/D_M$	0.125	59° (9°)	−8.60 (1.08)	2.13 (0.11)	5.02 (0.13)
$FH(M197)/T_w/D_M$	0.875	53° (10°)	−8.25 (1.46)	2.02 (0.13)	4.90 (0.16)
$FY(M197)/T_w/D_L$	0.125	47° (10°)	−5.95 (1.12)	2.23 (0.19)	4.67 (0.18)
$FY(M197)/T_w/D_L$	0.875	48° (11°)	−7.97 (2.76)	2.09 (0.15)	4.89 (0.27)
$FY(M197)/T_w/D_M$	0.125	47° (10°)	−9.14 (1.12)	2.00 (0.12)	5.27 (0.24)
$FY(M197)/T_w/D_M$	0.875	64° (12°)	−7.71 (0.88)	2.04 (0.10)	5.11 (0.14)
$FY(M197)/N_w/D_L$	0.125	58° (13°)	−7.13 (1.47)	2.08 (0.18)	4.84 (1.19)
$FY(M197)/N_w/D_L$	0.875	50° (76°)	−7.35 (1.52)	4.19 (1.23)	2.97 (1.04)

[a] The fluctuations of quantity x are evaluated as rms values according to $[\langle(x - \langle x\rangle)^2\rangle]^{0.5}$. [b] The data are based on dynamics simulation of 150 ps where the last 100 ps are used for analysis. In the left column the first entry refers to the mutant considered, the second entry to the structure used as the start conformation of the dynamics simulation, and the third entry indicates which of the two acetyl groups at the special pair is considered. [c] The special pair charges of 0.125 and 0.875 correspond to trajectories used for the FEP method and are the closest to the relevant special pair charges of the reduced (0) and oxidized (1) states. [d] The torsion angle of the acetyl group at the special pair as referenced in the first column is given. [e] The average interaction energy of the acetyl group atoms (Coulomb, Lennard-Jones, and torsion energy terms) is evaluated with respect to all atoms of the protein and cofactor environment. [f] Referring to the acetyl group at D_L [D_M] one considers the hydrogen bond to H(L168) [M197]. [g] The distance between to the Mg^{2+} ion of D_M [D_L] and the oxygen atom of the reference acetyl group at D_L [D_M], as indicated in the first column, third entry, is considered.

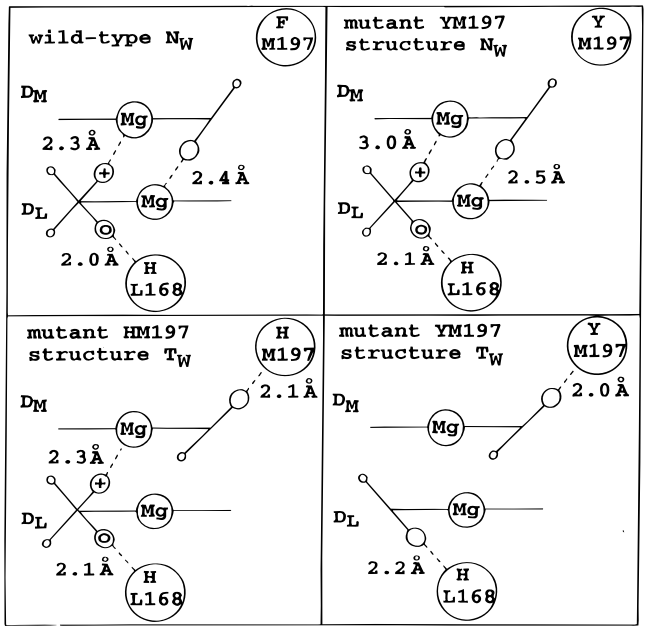

Figure 3. Average conformation of the acetyl groups at the special pair from dynamics simulation. The acetyl group orientations at the special pair are depicted schematically. The same viewpoint as in Figure 2 is used. The oxygen atoms of the acetyl groups are represented by the larger spheres. The zero (plus) sign in these spheres indicates the acetyl group orientation in the reduced (oxidized) special pair state. If the charge state of the special pair is not indicated, the orientation of the corresponding acetyl group changes only marginally with the redox state of the special pair. Hydrogen bonds and short distances to the Mg^{2+} ions are indicated by dashed lines. The average lengths of the hydrogen bond and oxygen Mg atom distances are evaluated from the last 100 ps of trajectories of 150 ps total simulation time used for the FEP method with $\lambda = 1/8$ ($\lambda = 7/8$) corresponding approximately to the reduced (oxidized) special pair state. Considered are the average wild-type RC in structure N_w (top left), the mutant FH(M197) RC in structure T_w (bottom left), and the mutant FY(M197) RC in structure N_w (top right) and in structure T_w (bottom right).

With the exception of the mutant FY(M197) the electrochemical shifts are larger for acetyl oxygen atoms than for keto oxygen atoms.[49]

The formation of hydrogen bonds between residues and the acetyl oxygen atoms requires specific orientations of the acetyl groups. In the wild-type structure of the *Rb. sphaeroides* RC, the acetyl oxygen atom at D_L points away from the Mg^{2+} ion of D_M and forms a hydrogen bond with H(L168). Although there is no hydrogen bonding partner for the acetyl oxygen atom at D_M, the electron density map exhibits a weak preference for a conformation of the acetyl group at D_M, where the oxygen atom points away from the Mg^{2+} ion of D_L.[5] This structure and all structures derived from it by energy minimization or dynamics simulation are denoted by n (normal). By rotating the acetyl group at D_M in structure n by 180° the acetyl oxygen atom binds to the Mg^{2+} ion of D_L. This structure and all structures derived from it are denoted by t (turned). Using the semiempirical energy function of CHARMM the conformation of the acetyl group at D_M in structure t where the oxygen atom binds to the Mg^{2+} ion of D_L is energetically more favorable than the acetyl group conformation in structure n (see Table 2).

The computations in the present and earlier work[16] are based on a preliminary structure of the RC of *Rb. sphaeroides* denoted henceforth by N. The main difference between structure n and N is in the orientation of the acetyl group at D_M. In structure N the acetyl oxygen atom points toward the Mg^{2+} ion of D_L similar to that in structure t. The corresponding counterpart to structure n is structure T where the acetyl group is rotated by 180° relative to the orientation in structure N. The equivalence of the pair of structures n and T (t and N) becomes evident after energy minimization. Using the weak torsion potential (eq 1) for the acetyl group at D_M the difference in the torsion angle between structure n and T (t and N) is only 8° (2°). For the strong torsion potential the corresponding difference of the acetyl group torsion angle at D_M is 7° (8°) (see Table 2). This structural similarity and the possibility of a more direct comparison with related computations[16,50] justifies the use of the structures N and T instead of t and n.

Orientation of Acetyl Groups from Dynamics Simulation: Wild-Type RC and Mutants YF(M210) and YF(L162). The

(49) Mattioli, T. A.; Williams, J. C.; Allen, J. P.; Robert, B. *Biochemistry* **1994**, *33*, 1636−1643.
(50) Ullmann, G. M.; Muegge, I.; Knapp, E. W. *Feldafing III Proceedings* **1996**, in press.

computer simulation of dynamics of the special pair environment of the RC allows for larger conformational changes than energy minimization. In the latter case, only minor adjustments of distances can occur, and sometimes, the minimization may stop in a side minimum, whose structure is not an appropriate representation of the considered mutant. In a dynamics simulation of the RC where the mobility of the molecular groups in the neighborhood of the special pair is not restricted by constraints, reorientations of small molecular groups can occur where hydrogen bonds break or form. It is this structural flexibility which can provide better agreement with the measured values of the shift of the special pair redox potential.

By starting the simulation of dynamics of the wild-type RC from structure N_w, the hydrogen bond between the acetyl oxygen atom at D_L and the residue H(L168) remains for the reduced (neutral) special pair state but breaks in a few picoseconds in the oxidized (positively charged) special pair state (see Figure 3, top left). If this hydrogen bond breaks, a new bond forms between the acetyl oxygen atom at D_L and the Mg^{2+} ion of D_M. The new bond with the Mg^{2+} ion is stronger than this hydrogen bond. See for instance the interaction energy of the acetyl group at D_L in structure N_w of the wild-type RC for the reduced and oxidized special pair state (first two lines in Table 3). This difference in interaction energy can be rationalized by the atomic partial charges, which are for the Mg^{2+} ion of D_M +0.396 (+0.414) for the reduced (oxidized) special pair state but only +0.30 for the hydrogen atom of the histidine H(L168). The orientation of the acetyl group at D_M remains regardless of the charge state of the special pair. Starting from the wild-type RC structure T_w, where the acetyl oxygen atom at D_M points away from the Mg^{2+} ion of D_L, this acetyl group reorients in a few picoseconds to form a bond with the Mg^{2+} ion of D_L regardless of the charge state of the special pair. At the same time the hydrogen bond between the acetyl oxygen atom at D_L and the N_ϵ nitrogen atom of residue H(L168) gets loose and the oxygen atom starts to fluctuate between this hydrogen bond and a bond which is formed with the Mg^{2+} ion of D_M (see Table 3). In a sense the structural character of the initial wild-type RC structure T_w which remains intact if only energy minimization is applied is lost during the initial part of the dynamics simulation. Hence, the values of the special pair redox potentials obtained from electrostatic and free energy computations which are based on the wild-type structure T_w cannot directly be compared.

In a dynamics simulation of the RC in structure N_w the mutant YF(L162) exhibits the same hydrogen bonding pattern with respect to the acetyl groups of the special pair as the wild-type RC. In particular, the hydrogen bond initially formed by the acetyl group at D_L and the histidine L168 breaks in the oxidized special pair state. The mutant YF(M210) shows a different behavior. Here the hydrogen bond between the acetyl oxygen atom at D_L and the residue H(L168) remains also in the oxidized special pair state. Dynamics simulations of the mutants YF(L162) and YF(M210) in structure T_w were not performed, since a reorientation of the acetyl group at D_M was expected similar to that for the corresponding wild-type structure. Using the strong torsion potential (eq 1) instead, the acetyl groups of the special pair are forced to orient in-plane with respect to their corresponding BChl monomers. In the T_s (or equivalently n_s) structure the acetyl oxygen atom at D_M has no significant bonding partner. Therefore, the acetyl group at D_M remains in the in-plane orientation (see Table 2). However, during the dynamics simulation, a weak hydrogen bond (heavy atom distance 3.8 Å) forms with the hydroxyl oxygen atom of the tyrosine M210. This hydrogen bond is weaker for the oxidized than for the reduced special pair state. The hydrogen bond between the acetyl oxygen atom at D_L and residue H(L168) remains intact in both redox states of the special pair. In structure N_s (or equivalently t_s) the acetyl group at D_M adopts an out-of-plane orientation, where the oxygen atom binds to the Mg^{2+} ion of D_L (Table 2). This bond remains intact also during dynamics simulation in the reduced and oxidized special pair state. In the mutants YF(L162) and YF(M210) with structure N_s the acetyl groups at the special pair behave similar to those in the corresponding structure of the wild-type RC. Dynamics simulations of these mutants in structure T_s were not performed.

Orientation of the Special Pair Acetyl Groups: The Mutants FH(M197), FY(M197), and FH(M197) + HF(L168). By starting the dynamics simulation of the mutant FH(M197) RC with the initial structure T_w, the hydrogen bonding scheme of the acetyl groups at the special pair does not change in the reduced (neutral) special pair state. In the oxidized (positively charged) special pair state the hydrogen bond between the acetyl oxygen atom at D_L and the residue H(L168) breaks in the first few picoseconds of the dynamics simulation (see Figure 3, bottom left) similarly to that for the wild-type RC in structure N_w. In structure T_s the initial hydrogen bonding pattern of the special pair does not change during the dynamics simulation. Dynamics simulations of the mutant FH(M197) in the structures N_w and N_s were not performed, since there is no experimental hint that the acetyl oxygen atom at D_M is not hydrogen bonded with H(M197).

Using the initial structure T_w for the dynamics simulation of the mutant FY(M197) RC, the hydrogen bonding scheme remains in the reduced and oxidized special pair state (Figure 3, bottom right). This is in contrast with mutant FH(M197), where the hydrogen bond between the acetyl oxygen atom at D_L and residue H(M197) breaks in the oxidized special pair state. With the initial structure N_w for the dynamics simulation of the mutant FY(M197) the hydrogen bond of the acetyl oxygen atom with the residue H(L168) breaks in the oxidized (positively charged) special pair state (Figure 3, top right). Thus the hydrogen bonding scheme of this mutant is equivalent to the one of the wild-type RC's (Figure 3, top left). A dynamics simulation of the mutant FY(M197) with the strong torsion potential was only performed for structure T_s. There the initial hydrogen bonding pattern did not change during the dynamics.

The relevant structure for the double mutant FH(M197) + HF(L168) is T_w, where the acetyl oxygen atom at D_M forms a hydrogen bond with the residue H(M197) as it does for the single mutant FH(M197). Also in the dynamics simulation of the double mutant the acetyl group at D_L reorients in the first few picoseconds such that the acetyl oxygen atom binds to the Mg^{2+} ion of D_M. No difference in the hydrogen bonding pattern can be observed between the reduced and oxidized special pair state. The hydrogen bonding pattern of the double mutant in structure T_s is similar to the one in structure T_w. Dynamics simulation of the double mutant in structure N_w and N_s was not performed.

Summary and Interpretation of Structural Changes. The following structural changes of the special pair acetyl groups occur during dynamics simulation:

(1) Starting from structure T_w for the wild-type RC and the mutants where no hydrogen bond is formed with the acetyl oxygen atom at D_M, the acetyl group at D_M reorients during the initial part of the dynamics simulation to form a bond with the Mg^{2+} ion of D_L. Using N_w as the initial structure for the dynamics simulation the bond of the acetyl oxygen atom at D_M with the Mg^{2+} ion of D_L has already formed.

(2) By starting a dynamics simulation from structure N_w the hydrogen bond between the acetyl oxygen atom at D_L and the residue H(L168) remains in the reduced (neutral) special pair state for the wild-type and all mutant RC's and breaks for the oxidized (positively charged) special pair state, except for the mutant YF(M210). The same happens for the mutant FH-(M197) RC starting from structure T_w.

(3) In structure T_w the initial hydrogen bonding pattern of the two acetyl groups at the special pair of the mutant FY-(M197) does not change during dynamics simulation. In particular, the hydrogen bond between the acetyl oxygen atom at D_L and the residue H(L168) remains also for the oxidized (positively charged) special pair state.

(4) The hydrogen bond formed in structure T_w between the acetyl oxygen atom at D_M and the residue H(M197) in the corresponding mutants remains intact during dynamics simulation independent of the charge state of the special pair.

With the exception of observation 3 these structural changes can qualitatively be understood by considering the Coulomb interactions of the acetyl oxygen atoms. For the wild-type RC and the mutants YF(L162) and YF(M210) there is no competition with the strong Coulombic attraction of the acetyl oxygen atom at D_M and the Mg^{2+} ion of D_L, leading to the conformational change observed in the dynamics simulation (observation 1).

In the oxidized state the atomic partial charges of the special pair oxygen atoms are charged less negative than in the reduced special pair state. Consequently the hydrogen bonds involving the acetyl groups of the special pair are less stable in the oxidized than in the reduced state and should break preferentially in the oxidized state of the special pair. See for instance the interaction energy of the acetyl groups at D_M in structure T_w. This energy is for the mutant FY(M197) [(FH(M197)] about 1.4 kcal/mol (0.35 kcal/mol) higher in the oxidized than in the reduced state (Table 3). From the difference in pK_a values it can be concluded that a hydrogen bond with the hydroxyl group of tyrosine is stronger than with the imidazole ring of a neutral histidine. This explains the above-mentioned energy difference. In the CHARMM force field this effect is accounted for by the atomic partial charge of the hydrogen atom which is +0.4 for tyrosine and only +0.3 for histidine.[28] All this corroborates the observation 1 made in the dynamics simulation. It is however in contrast with mutant FY(M197) in structure T_w, where the hydrogen bond between the acetyl oxygen atom at D_L and residue H(L168) remains also in the oxidized special pair state (observation 3). According to Table 3 for this mutant the hydrogen bond is about 2 kcal/mol stronger in the oxidized than in the reduced special pair state. This may be due to other structural rearrangements. The presence of the strong hydrogen bond of the acetyl oxygen atom at D_M may have a stabilizing effect on the hydrogen bond with the acetyl oxygen atom at D_L. The asymmetry of the charge distribution (0.28 at D_M^+ and 0.72 at D_L^+) in the oxidized special pair state weakens in particular the hydrogen bond of the acetyl oxygen atom at D_L. This is in agreement with the results from computer simulations where the hydrogen bonds remain at D_M (observation 4) and break at D_L (observation 2).

Shifts of the Special Pair Redox Potential Evaluated by Computer Simulation of Free Energy. The FEP method[17−20] is used to calculate the shift of the redox potential for a selection of single-point mutants YF(L162), YF(M210), FY(M197), and FH(M197) and the double mutant FH(M197) + HF(L168) (listed in Table 1) as described in the Methods. Preferentially, mutants are considered where the computation of electrostatic energies by solving Poisson's equation faces problems (first two mutants) or where changes in the hydrogen bonding scheme of the acetyl group at D_M occur (last three mutants). Mutants where the distribution of atomic partial charges at the special pair changes drastically are not considered, since only the wild-type atomic partial charges are available. These changes were observed for instance for the mutants, where a hydrogen bond at the ring V keto oxygen atoms was added.[27]

The computations with the FEP method require up to 2 ns of dynamics simulations to obtain a single value of the shift of the redox potential. Therefore, not for all combinations of the wild-type and mutant structures are the shifts of the redox potential evaluated. The results marked in bold type in Table 1 refer to the wild-type structure N_w. For the mutants they refer to structure T_w if the acetyl oxygen atom at D_M is known to form a hydrogen bond (mutants FY(M197) and FH(M197) and the double mutant) or to structure N_w if the acetyl oxygen atom at D_M is not involved in a hydrogen bond (mutants YF(L162) and YF(M210)). With the exception of the single-point mutation FY(M197) the corresponding calculated values of the shift of the special pair redox potential agree well with experimental data. Other combinations of wild-type and mutant structures used for the free energy computations are less successful.

Appropriate values of the shift of the redox potential are also obtained for the first two mutants using the wild-type structure T_s and the mutant structures N_s with the strong torsion potential. However, these mutants do not add a hydrogen bond to the acetyl oxygen atom at D_M. Therefore, a change in the acetyl group conformation at D_M going from the wild-type to the mutant structure of the RC cannot well be motivated. The only other agreement between calculated and experimental shifts of the redox potential is obtained for the mutant FY(M197) using the structure T_s (strong torsion potential) for the mutant and wild-type RC. However, the same combination of structures fails for mutant FH(M197) and the double mutant. Hence, the calculated shifts of the special pair redox potential using the FEP method clearly favor the weak torsion potential.

The values of the shift given in Table 1 show a regularity which can be expressed by the relation $\Delta\Delta E_M(T^{WT}-N^{WT}) = \Delta E_M(T^{WT},X^{mut}) - \Delta E_M(N^{WT},X^{mut}) = \text{constant} > 0$. The arguments of ΔE_M refer to the different wild-type structures T^{WT} and N^{WT} but the same mutant structure X^{mut}, where X can be N or T. The constant values of $\Delta\Delta E_M(T^{WT}-N^{WT})$ assume, independent of the mutant considered, the value 38 mV for the weak and 96 mV for the strong torsion potential. This relation can be traced back to the free energy difference of the wild-type RC $\Delta G^{WT}(T) - \Delta G^{WT}(N) > 0$, since the contribution of the corresponding mutant cancels in expression $\Delta\Delta E_M(T^{WT}-N^{WT})$. The inequality $\Delta G^{WT}(T) > \Delta G^{WT}(N)$ tells us that in structure T of the wild-type RC the free energy is more sensitive to changes of the special pair charge state than in structure N. This can be understood from the difference in the two structures. In structure T both acetyl oxygen atoms of the special pair bind to the corresponding Mg^{2+} ion and can thus sense the change in the atomic partial charge directly. In structure N only the acetyl oxygen atom at D_M binds to its corresponding Mg^{2+} ion.

Shift of the Special Pair Redox Potential Evaluated with DelPhi. By solving Poisson's equation for the energy-minimized structures of the wild-type and mutant RC only for the two mutants involving the point mutation FH(M197), agreement with the experimental shift of the redox potential was possible.[16] The first three mutants YF(L162), YF(M210), and FY(M197) were not considered before. For these mutants no combination of mutant and wild-type RC structure used for the solution of Poisson's equation could reproduce the experi-

mental values of the shift of the redox potential. Table 1 (last column) displays only the shifts of the redox potential calculated with DelPhi for the structures which agree with the assumed hydrogen bonding pattern of the acetyl groups at the special pair (bold numbers in column 1 and 2 of Table 1). For the first two mutants the hydrogen bonding pattern is assumed to be the same as for the wild-type RC. Nevertheless, the shift calculated with DelPhi is in one case [YF(M210)] 100 mV, a value typical for the formation of a hydrogen bond in the mutant. A close inspection of the energy-minimized structures, which are used for the computation of this shift, reveals no change in the bonding scheme. No other specific reason for this deviation could be found. Apparently the energy-minimized structures of the RC and its mutants, which are all very close to the crystal structure, are in this case not suitable to obtain the appropriate value for the shift of the redox potential. On the other hand, the FEP method which includes also structural fluctuations is able to reproduce the experimental values of the shift.

The Mutant FY(M197). The mutant FY(M197) was designed to establish an additional hydrogen bond between the acetyl oxygen atom at D_M and the hydroxyl group of the tyrosine. In the resonance Raman spectrum of the special pair one observes, comparing the wild-type RC and the mutant FY(M197), a red shift of a vibrational band whose frequency corresponds to an acetyl group.[24] The frequency shift of this band is 17 cm^{-1}, which is only one-half as large as expected from the formation of a strong hydrogen bond. The measured upshift of the redox potential for this mutant is with 31 mV also too small for the formation of a regular hydrogen bond. The corresponding hydrogen bond of the mutant FH(M197) leads to an upshift of the redox potential whose experimental value is 125 mV. With FEP calculations using the mutant structure T_w the special pair redox potential yields an upshift of 127 mV for the mutant FY(M197) and 94 mV for FH(M197).

In the dynamics simulation the hydrogen bond of the acetyl oxygen atom and residue M197 is stronger with a tyrosine than with a histidine mutant. Therefore, the tyrosine mutant yields a larger upshift of the redox potential. This is also obvious from the atomic partial charge of the polar hydrogen atom used in CHARMM22, which is 0.1 elementary charge larger for tyrosine than for histidine. Correspondingly in the reduced special pair state the interaction energy of the acetyl group at D_M is lower and the hydrogen bond distance is smaller if residue M197 is mutated to tyrosine rather than to histidine (see Table 3). This cannot be observed for the oxidized special pair state and must be due to differences in the average structure of the two mutants not involving the acetyl group at D_M directly. For the energy-minimized structures which are used for the computation of electrostatic energies also in the reduced special pair state the interaction energy of the acetyl group at D_M is slightly lower for the histidine than the tyrosine mutant. No explicit data are shown for this case.

In the structure T_w the orientations of the acetyl groups (at D_L and D_M) of the mutant FY(M197) are exceptional. In contrast to all other considered mutants including the wild-type RC the hydrogen bonds of both acetyl oxygen atoms at the special pair remain intact even in the oxidized state if the weak torsion potential is applied. Since in this case the hydrogen bonding pattern does not change during the dynamics simulation, it is not surprising that the shift of the redox potential calculated with the FEP method correlates well with the value of 96 mV obtained by solving Poisson's equation for the corresponding energy-minimized structures. The structure T is supported by the resonance Raman spectrum of the mutant FY(M197).[24] Nevertheless the experimental value of the shift of the redox potential is too low for the formation of a hydrogen bond. It is however typical for the change from a hydrophobic to a more polar special pair environment similar to that observed for the mutants FY(M210) and FY(L162) (see Table 1). The FEP computations yield a shift of the special pair redox potential which agrees with the experimental value only if the mutant structure N_w is used, where the acetyl oxygen atom is not hydrogen bonded to the tyrosine M197. On the other hand, for the mutant FH(M197), agreement is obtained with structure T_w, though the corresponding hydrogen bond should be weaker for the histidine than for the tyrosine mutant. The bond of the acetyl oxygen atom at D_M with the Mg^{2+} ion in structure N_w should have about the same strength as the hydrogen bond with the hydroxyl group of the tyrosine M197 in structure T_w. A more direct estimate on the role which the structures T_w and N_w play for the mutant FY(M197) can be obtained from a computation of the free energy difference between these structures. This requires performance of a computer simulation of the dynamics with a constrained orientation of the considered acetyl group at D_M, which will be done in future work.

Conclusions

The shifts of the special pair redox potential of the RC *Rb. sphaeroides* were calculated for five different mutants and compared with experiments. Two different methods were used. The method based on computations of electrostatic energies by solving Poisson's equation of energy-minimized structures of the RC succeeds only for two out of five mutants. The second method uses dynamics simulation data to calculate free energy differences. This method yields a proper value of the shift of the special pair redox potential for all mutants considered except for mutant FY(M197). By orienting the acetyl group at D_M such that the oxygen atom points toward the Mg^{2+} ion of D_L (structure N) for the wild-type RC and the mutant FY(M197), agreement with the experimental value of the shift of the redox potential is also obtained for this mutant.

Since the acetyl group orientations at the special pair determined by crystal structure analysis are not so certain, the orientation of the acetyl group at D_M, which is the BChl of the inactive branch, is varied. Two different initial acetyl group conformations are considered for the wild-type and mutant RC. In one conformation (T), the acetyl oxygen atom at D_M points away from the Mg^{2+} ion of D_L (original crystal structure); in the second conformation (N), the acetyl oxygen atom binds to the Mg^{2+} ion of D_L. Furthermore, to allow for better reorientation of the acetyl groups, the value of the force constant of the torsion potential is lowered.

The FEP method requires about 2 orders of magnitude more CPU time than is needed by solving Poisson's equation. It therefore cannot routinely be applied to many mutants. During the dynamics simulation which provides the raw data for the FEP method, conformational changes may occur such that the average conformation can differ from the initial conformation in important details. Often changes in the hydrogen bonding pattern are observed which have a strong influence on the calculated shift of the redox potential. Such changes are not possible with the method of energy minimization where structural details taken from the crystal structure remain. As a consequence new structural features which can be in conflict with the interpretation of experimental data occur more easily with dynamics simulation than by using energy minimization. According to the success of the FEP method for this problem the structural flexibility seems to be more important than a proper treatment of the electrostatic energies for an inhomogeneous dielectric medium. The new structural features are as

follows: (1) In the wild-type structure the acetyl oxygen atom at D_M points to the Mg^{2+} ion of D_L instead of pointing away as in the crystal structure.[5] (2) In contrast to the findings from resonance Raman spectra[24] the acetyl oxygen atom at D_M does not form a hydrogen bond with residue Y(M197) but points to the Mg^{2+} ion of D_L. (3) The hydrogen bond between the acetyl oxygen atom at D_L and residue H(L168) which is present in the reduced state is broken in the oxidized special pair state. Instead the oxygen atom binds to the Mg^{2+} ion of D_M. However, ENDOR spectra can be interpreted without invoking these structural changes.[23] (4) The strength of the torsion potential of the acetyl groups is rather small.

A major uncertainty of the present computations are the values of the atomic partial charges of the special pair. In the present treatment these are not adjusted to the different orientations of the acetyl group. However, it is known that the atomic charges of the acetyl group atoms can depend critically on the orientation of the acetyl group.[42] Furthermore the charges must be adjusted to the different mutants. Especially for the dynamics simulations, this requires a large amount of quantum chemical calculations of high precision applied to large systems and must therefore be postponed for some time. Another aspect is that it might also be useful to check on the interpretations of some of the experiments where conflicts arise.

Acknowledgment. The authors thank Professors Hartmut Michel and Wolfgang Lubitz for valuable discussions. We are grateful to Dr. Martin Plato, Dr. Philipp Scherer, and Bernd Melchers for calculating the atomic partial charges of the cofactors. The CHARMM source code has been provided by Professor Martin Karplus and Molecular Simulations Inc. This work is supported by the Deutsche Forschungsgemeinschaft SFB 312, Projekt D7, and the Fonds of the Deutsche Chemische Industrie.

JA9535219